

Investigating the Effect of Process Parameters on Reducing the Peeling Stress in Adhesive Joints of Composite Materials

Saeed Yaghoubi¹, *

Department of Mechanical Engineering, Faculty of Engineering,
Ilam University, Ilam, Iran

E-mail: S.yaghoubi@ilam.ac.ir

*Corresponding author

Mohammad Shishesaz², Kiamehr Rouzbakhshzadeh³

Department of Mechanical Engineering, Faculty of Engineering,
Shahid Chamran University of Ahvaz, Ahvaz, Iran

E-mail: Mshishesaz@scu.ac.ir, Kiamehr67@gmail.com

Received: 19 October 2022, Revised: 18 January 2023, Accepted: 20 January 2023

Abstract: Joints are considered the weakest part of an engineering structure and failure usually occurs in this region, firstly. One of the main factors in the rupture of adhesive joints is the normal stresses between the layers created by the presence of an out-of-center load and bending moment. The present research work has focused on the influence of parameters including the adhesive zone length, adhesive and adherend layer thickness on reducing the amount of normal interlayer stress in a single-lap adhesive joint. Optimization of parameters have been done using BA and PSO optimization algorithm. The distribution of normal and shear stresses are based on two-dimensional elasticity theory that includes the complete stress-strain and strain-displacement relations for the adhesive and adherends. The results obtained from current research revealed that by optimization of mentioned parameters, the value of peeling stress is significantly reduced. Although increasing in Young's modulus of adhesive layer leads to an increase in normal stress of the joint, it creates a more uniform stress distribution at the edges. The outcomes also revealed that increasing the length of the joint zone and the thickness of adherends can improve the interlayer normal stress in the adhesive joint.

Keywords: Adherend, Adhesive, Adhesive Joint, Interlayer Normal Stress, Optimization Algorithms

Biographical notes: **Saeed Yaghoubi** is Assistant Professor of Mechanical Engineering at Ilam University, Ilam, Iran. He received his PhD in Mechanical Engineering from Bu-Ali Sina University, in 2020. **Mohammad Shishesaz** is professor of Mechanical Engineering at Shahid Chamran University of Ahvaz, Ahvaz, Iran. He received his PhD in Mechanical Engineering from Northeastern University, in 1986. **Kiamehr Rouzbakhshzadeh** received his MSc in Mechanical Engineering from Shahid Chamran University of Ahvaz, in 2013.

Research paper

COPYRIGHTS

© 2023 by the authors. Licensee Islamic Azad University Isfahan Branch. This article is an open access article distributed under the terms and conditions of the Creative Commons Attribution 4.0 International (CC BY 4.0)

<https://creativecommons.org/licenses/by/4.0/>



1 INTRODUCTION

Composite material is the combination of at least two different substances on a macroscopic scale to obtain a new material. These materials are widely used in industries such as electrical, automotive and aerospace industries. Each layer of composite material may have different mechanical, physical and chemical properties. Therefore, properties such as high yield strength, fracture resistance, electrical conductivity, etc., which may not exist in a single metal, can be obtained by combining materials [1-3]. In many situations, it may not be possible to create a completely composite structure. Among these cases, connecting two non-homogeneous materials or making geometries that cannot be produced in one piece can be mentioned. Therefore, the connection between two or more substances is inevitable. Connections are almost the biggest cause of failure in the parts of aerial structures, and therefore it is very important to pay attention to all parameters and their design during the design of the structure [4]. Nowadays, there are three main methods for connecting composite materials to themselves or other materials such as metals, ceramics, plastics, etc., which include mechanical connections, adhesive connections, and a combination of these two types. Adhesive joints of composite materials can be designed in such a way that the adhesive can tolerate loads greater than the strength of the original material and the designed joints do not fail due to the application of fatigue loads [5-6]. Considering the wide application of adhesive joints of composite materials in various industries, it seems necessary to study the behavior of these materials. Although the appearance of the structure of most joints seems simple, but due to the existence of several different layers and the possibility of using different materials in the layers, the mechanical behavior and their analysis and optimal design are very complex. Therefore, due to the lack of comprehensive analytical solutions, this category has received less attention and most of the previous works in this field have been done using numerical methods or practical experiments. Adhesive joints may be preferred in cases where a narrow part of the structure must be connected and the bearing stress in the mechanical connection is high (or the weight of the mechanical connection exceeds the permissible limit). Uniform stress distribution along the adhesive area due to high contact surface, high resistance to fatigue and corrosion, high strength-to-weight ratio and reasonable price are prominent features of adhesive joints. In the design of these connections, it is necessary to pay attention to the fact that the shape of the connection is chosen in such a way that the stress on the adhesive appears in shearing form. Adhesives are highly vulnerable to normal stresses. If the normal stresses

between the layers are large, they lead to the separation of the adhesive layer from the adherend, which is called peeling stress. It is impossible to remove all the normal stresses that cause the peeling effect on the connection surface. The main reason for the occurrence of peeling stress in the joint surface is the presence of an Eccentricity load produced into the connection, which itself causes the bending moment and, as a result, the normal stress. The amount of this stress can be controlled and optimized by applying changes in the dimensions and ratio of length and thickness of the adhesive.

In the field of adhesive joints of composite materials, several researches have been done. Zhao and Lu [7], based on two-dimensional elasticity relations and equilibrium Equations, obtained a package solution for determining the stress and strain in the middle surface of the adhesive and the interlayer stress in the interface between the adhesive and the adherend layers. Bavi et al. [8] studied the geometrical optimization of the single-lap adhesive joint consisting of mixed adhesive using genetic and bees algorithms. The objective parameters in their research included maximizing the applicable load and special resistance of the joint. Shishehsaz et al. [9] studied the transient stress distribution in single-lap adhesive joints. In their study, the Equations were extracted based on Shear Lag's theory and the Equations were solved based on the explicit finite difference method. Salahi et al. [10] investigated the transient dynamic analysis of semi-analytical type for single-lap adhesive joint. The results obtained in their research were validated through comparison with the experimental outcomes of previous research. Wang et al. [11], studied the effect of loading rate on the mechanical behavior and failure of single-lap adhesive joints. The results of their investigation demonstrated an increase in the shear strength of the joint as a result of increasing the loading rate. Miguel et al. [12] evaluated the three-dimensional stress field created in the adhesive joint using a high-order numerical simulation model. The accuracy of the model presented in their study was checked through comparison with the analytical and numerical solutions available in the previous references. Polini et al. [13] evaluated the effect of misalignment of adherends on adhesive bond strength. In another study, Beigezaee et al. [14] improved the strength of single-lap adhesive joint via using notching technique. In this method, they created a rectangular and semicircular cut on the outer surface of the adherend and observed the improvement of the joint strength. Peres et al. [15] investigated the geometry and adhesive optimization in single-edge adhesive joint under impact. The results of their research showed that with the increase in overlap length, the strength of the joint increases, especially for flexible adhesives. Marchione [16] analyzed the effect

of hollow adherends on reduction of peak stress in single-lap adhesive joints using finite element and analytical solutions. The results of their study demonstrated that the maximum reduction of peak stress is observed at section with maximum slot on both adherends.

Based on the previous studies presented in current section, it can be seen that adhesive joints are of special importance and have various applications in the different industry. One of the most important defects in the mentioned joints is the peeling stress, which has not received much attention in previous researches. In the present research work, optimization of parameters in order to attain maximum reduction in interlayer normal stress has been performed. The parameters studied in current research include the adhesive zone length, adhesive and adherend layer thickness. The examined composite material consists of a symmetrical single-lap joint that is affected by tensile force in the longitudinal direction. It should be noted that the behavior of adhesive joint components is considered in the linear elastic range.

2 RELATIONSHIPS GOVERNING SINGLE-LAP ADHESIVE JOINT

The purpose of current section is to extract the governing relationships of composite single-lap adhesive joint using two-dimensional elasticity theory, stress-strain and strain-displacement relationships in order to investigate the stress distribution in the bonding layers. For this purpose, a view of a single-lap adhesive joint is shown in "Fig. 1". In this adhesive joint, two adherends with t_1 and t_2 thicknesses are connected via an adhesive layer with thickness of t_3 . As it is clear in the mentioned figure, the two free ends of the connection components are on a simply support and tolerate the tensile force (F). The parameters include μ_i ($i=1,2,3$), G_i and Poisson's ratio, shearing E_i modulus, and Young's modulus for the upper layer, lower layer, and adhesive layer, respectively. It should be mentioned that the length of the adhesive area and the non-adhesive areas are considered to $2l$ and L , respectively.

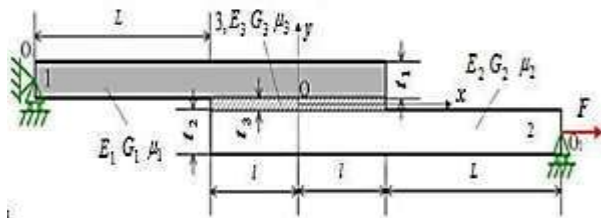


Fig. 1 Two-dimensional model of single-lap joint.

1. The stress state is considered as plane-stress.
2. The bonded layers and the adhesive layer are considered isotropic.
3. The shear stress along the thickness of the adhesive is considered constant.
4. The Equation of longitudinal and transverse displacement changes in the adhesive layer are considered as a linear function in the direction of thickness.
5. The axial force in the adhesive has been omitted, which is a reasonable assumption considering the low Young's modulus of the adhesive compared to the adherend layers.
6. Cylindrically bent plate theory has been used in calculating the deflection in the adhesive area and adherend layers.

Based on the joint presented in the "Fig. 1", $\sigma_{ix}, \sigma_{iy}, \tau_i$ ($i=1,2,3$) and $\varepsilon_{ix}, \varepsilon_{iy}, \gamma_i$, the stresses and strains related to the three layers mentioned in the connection and σ_{3y}^u and σ_{3y}^l are respectively the peeling stress in the upper and lower levels of the adhesive layer. The parameter $\tau_3 = \tau_3(x) = \tau_m$ is average shear stress in the adhesive (the shear stress in the adhesive is assumed to be constant) and f_i ($i=1,2,3$), Q_i and M_i are respectively tensile force, shearing force and bending moment in each of the three joint components. Q_i^* ($i=1,2$) and M_i^* are shear force and bending moment at the ends of the two upper and lower components of the connection, which are also called edge loads ("Fig. 2"). Other edges of the connection are stress-free.

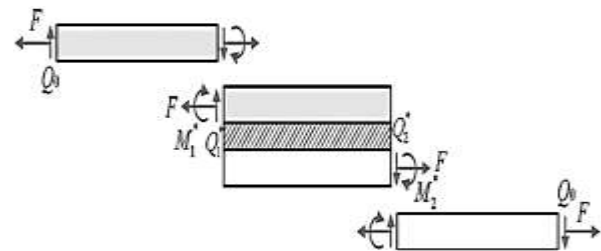


Fig. 2 Free body diagram of force balance in the single-lap joint.

The free body diagram for a small element of the joint region is shown in "Fig. 3". Based on the mentioned figure, the general equilibrium Equations (respectively along the x, y and z axis) and the boundary conditions are extracted as relations (1) to (4), respectively [17]. According to "Fig. 2", the general boundary conditions of the joint are obtained from the balance of edge loads in the form of Equation (4).

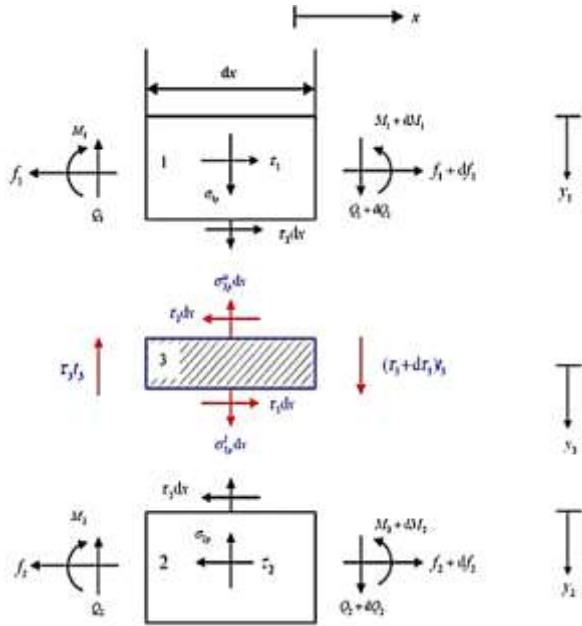


Fig. 3 Free body diagram of stress balance in the element in the adhesive joint region.

$$\frac{df_1}{dx} + \tau_3 = 0 \quad (1-a)$$

$$\frac{df_2}{dx} - \tau_3 = 0 \quad (1-b)$$

$$\frac{dQ_1}{dx} + \sigma_{3y}^u = 0 \quad (2-a)$$

$$\frac{dQ_2}{dx} - \sigma_{3y}^l = 0 \quad (2-b)$$

$$\frac{d\tau_3}{dx} t_3 - (\sigma_{3y}^u - \sigma_{3y}^l) = 0 \quad (2-c)$$

$$\frac{dM_1}{dx} - Q_1 + \tau_3 \frac{t_1}{2} = 0 \quad (3-a)$$

$$\frac{dM_2}{dx} - Q_2 + \tau_3 \frac{t_2}{2} = 0 \quad (3-b)$$

$$x = -l \Rightarrow M_1 = M_1^*, Q_1 = Q_1^*, f_1 = F, M_2 = Q_2 = f_2 = \tau_3 = 0 \quad (4-a)$$

$$x = +l \Rightarrow M_2 = -M_2^*, Q_2 = Q_2^*, f_2 = F, M_1 = Q_1 = f_1 = \tau_3 = 0 \quad (4-b)$$

In order to evaluate the edge loads, the bending stiffness of the layers should be calculated, firstly. To calculate this parameter, the distance between the neutral axis and the middle surface of the joint (the middle of the adhesive layer) must be obtained. To find the location of the neutral axis, it is integrated from the axial stress in the joint at an arbitrary cross-section in the form of Equation (5).

$$\sum F_x = \int_{-(t_2+d)}^{-d} \sigma_x dy + \int_{-d}^0 \sigma_x dy + \int_0^{(t_1-d)} \sigma_x dy = 0 \quad (5)$$

Considering the linear distribution of normal stress in the thickness of the connection, the distance of the neutral axis is derived in the form of Equation (6):

$$d = \frac{1}{2} \left(\frac{E_1 t_1^2}{1 - \mu_1^2} - \frac{E_2 t_2^2}{1 - \mu_2^2} \right) \times \left(\frac{E_1 t_1}{1 - \mu_1^2} + \frac{E_2 t_2}{1 - \mu_2^2} \right)^{-1} \quad (6)$$

Equation (7) is obtained by calculating the bending moment to evaluate the bending stiffness of the layers and the adhesive region. With this regard, D_1 and D_2 are respectively the bending stiffness of layers No.1 and No.2 in the non-adhesive region and D_3 is the bending stiffness in the adhesive region.

$$D_1 = \frac{E_1 t_1^3}{12(1 - \mu_1^2)} \quad (7-a)$$

$$D_2 = \frac{E_2 t_2^3}{12(1 - \mu_2^2)} \quad (7-b)$$

$$D_3 = \frac{E_1}{3(1 - \mu_1^2)} [(t_1 - d)^3 + d^3] + \frac{E_2}{3(1 - \mu_2^2)} [(t_2 + d)^3 - d^3] \quad (7-c)$$

In order to calculate the edge moments, one should first obtain the deflection relationship in different areas of the joint. Then, according to the cylindrically bent plate theory and using the relationship between moment and deflection (w) presented in Equation (8), edge moment to be evaluated.

$$\frac{d^2 w_i}{dx_i^2} = -\frac{M_i}{D_i} \quad (i = 1, 2, 3) \quad (8)$$

By applying the force boundary conditions governing the joint, the amount of shear force and bending moment are obtained as Equations (9) and (10), respectively.

$$Q_1^* = -D_1 \frac{d^3 w_1}{dx_1^3} \Big|_{x_1 = L_1} \quad (9-a)$$

$$Q_2^* = -D_2 \frac{d^3 w_2}{dx_2^3} \Big|_{x_2 = 0} \quad (9-b)$$

$$M_1^* = -D_1 \frac{d^2 w_1}{dx_1^2} \Big|_{x_1 = L_1} \quad (10-a)$$

$$M_2^* = -D_2 \frac{d^2 w_2}{dx_2^2} \Big|_{x_2 = 0} \quad (10-b)$$

The longitudinal normal stress (σ_{ix} ($i=1,2$)) in the joint components can be assumed to be linear along the thickness and expressed as Equation (11). The longitudinal normal stress in the adhesive has been omitted [18].

$$\sigma_{ix} = \frac{f_i}{t_i} + \frac{6M_i(2\rho_i - 1)}{t_i^2} \quad 0 \leq y_i \leq t_i, \rho_i = \frac{y_i}{t_i} \quad (11)$$

According to the two-dimensional elasticity relations, the stress components in the mentioned Equation must satisfy the equilibrium Equations presented in Equation (12):

$$\frac{\partial \sigma_{ix}}{\partial x} + \frac{\partial \tau_i}{\partial y_i} = 0 \quad (i=1,2,3) \quad (12-a)$$

$$\frac{\partial \sigma_{iy}}{\partial y_i} + \frac{\partial \tau_i}{\partial x} = 0 \quad (i=1,2,3) \quad (12-b)$$

By placing Equation (11) in the equilibrium Equations and also considering the shear stress continuity conditions between the adhesive and adherends and the conditions of the free surface above and below the bonding layers, the shear stress components are extracted as Equation (13).

$$\tau_1 = \tau_3(3\rho_1^2 - 2\rho_1) - 6Q_1(\rho_1^2 - \rho_1)/t_1 \quad (13-a)$$

$$\tau_2 = \tau_3(3\rho_2^2 - 2\rho_2 + 1) - 6Q_2(\rho_2^2 - \rho_2)/t_2 \quad (13-b)$$

By performing similar process, the normal stress components for adhesives layers are obtained as Equation (14):

$$\sigma_{1y} = \frac{d\tau_3}{dx}(-\rho_1^3 + \rho_1^2) + \sigma_{3y}^u(-2\rho_1^3 + 3\rho_1^2) \quad (14-a)$$

$$\sigma_{2y} = \frac{d\tau_3}{dx}(-\rho_1^3 + 2\rho_2^2 - \rho_2) - \sigma_{3y}^l(2\rho_2^3 - 3\rho_2^2 + 1) \quad (14-b)$$

$$\sigma_{3y} = \sigma_{3y}^u - \frac{d\tau_3}{dx}t_3(\rho_3 + 0.5) \quad (14-c)$$

It should be mentioned that in the above Equations, ρ_i ($i=1,2,3$) are the dimensionless thickness of the layers and it is presented in Equation (15):

$$0 \leq \rho_i \left(= \frac{y_i}{t_i} \right) \leq 1 \quad (i=1,2) \quad (15-a)$$

$$-0.5 \leq \rho_3 \left(= \frac{y_3}{t_3} \right) \leq 0.5 \quad (15-b)$$

3 OPTIMIZATION OF THE PROCESS

The aim of using optimization algorithms is to obtain the optimal amount of the objective parameter via considering the constraints of the problem and finding suitable values for the variables in a process. In present research work, the purpose is to use evolutionary algorithms based on the search method. As one of the methods of solving problems, these algorithms, inspired by natural evolution, are able to find the optimal answer and perform complex and time-consuming calculations that the traditional optimization methods often cannot answer. With this regard, among the existing algorithms, bees and particle swarm algorithms have been selected to perform the optimization operation. The main focus is on the bees algorithm, which is much newer, and in order to check the speed and accuracy of it, the outcomes of both methods will be compared with each other.

3.1. Bees Optimization Algorithm (BA)

Bees algorithm is a group based search algorithm that was first developed in 2005. This algorithm is simulating the food search behavior of bees groups. In the initial version of BA, the algorithm performs a type of local search that is combined with random search and can be used for combined optimization (simultaneous optimization of several variables) or functional optimization [19]. The flowchart related to the bees algorithm is shown in "Fig. 4". The main inputs of the bees algorithm for the current research are given in "Table 1".

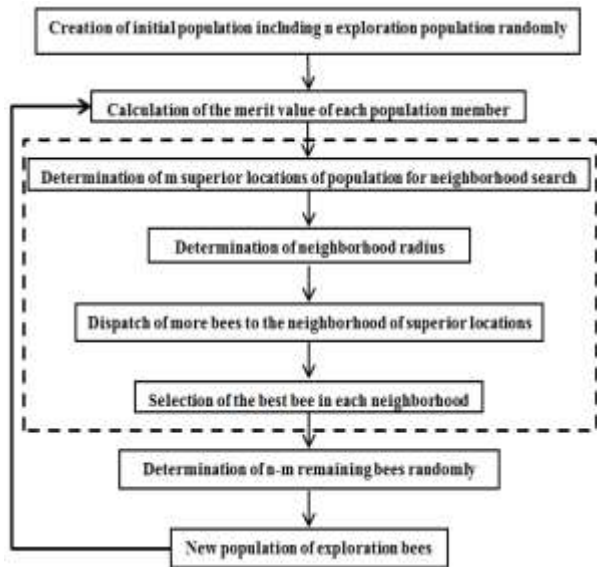


Fig. 4 Flowchart of bees optimization algorithm.

Table 1 Inputs of the bees optimization algorithm.

Parameters	Values
Population (n_{bees})	50
Number of selected sites (m)	20
Number of top-rated sites out of m selected sites (e)	5
Number of bees recruited for best e sites (n_{ep})	10
Number of bees recruited for the other ($m-e$) selected sites (n_{sp})	20
Initial rose-garden size (n_{gh})	$(x_j^{max} - x_j^{min}) / 50$
The number of objective function calculations	2000

3.2. Particle Swarm Optimization Algorithm (PSO)

The idea of particle swarm optimization was first proposed by Kennedy and Eberhart in 1995. Particle Swarm Optimization (PSO) is a social search algorithm that has been modeled on the social behavior of bird classes. At first, this algorithm was applied to detect the dominant patterns on the simultaneous flight of birds and sudden change of their trajectory and the optimal shape of the band. In this algorithm, the particles are flowing in the search area. Changing in location of the particles in the search area is under the influence of their own experience and knowledge and their neighbors. Thus, the position of other particles has effect on search method of a particle. The result of modeling this social behavior is searching process that will tend towards successful areas [20]. The flowchart for this optimization process is presented in “Fig. 5”. The main input of the particle swarm optimization algorithm is illustrated in “Table 2”.

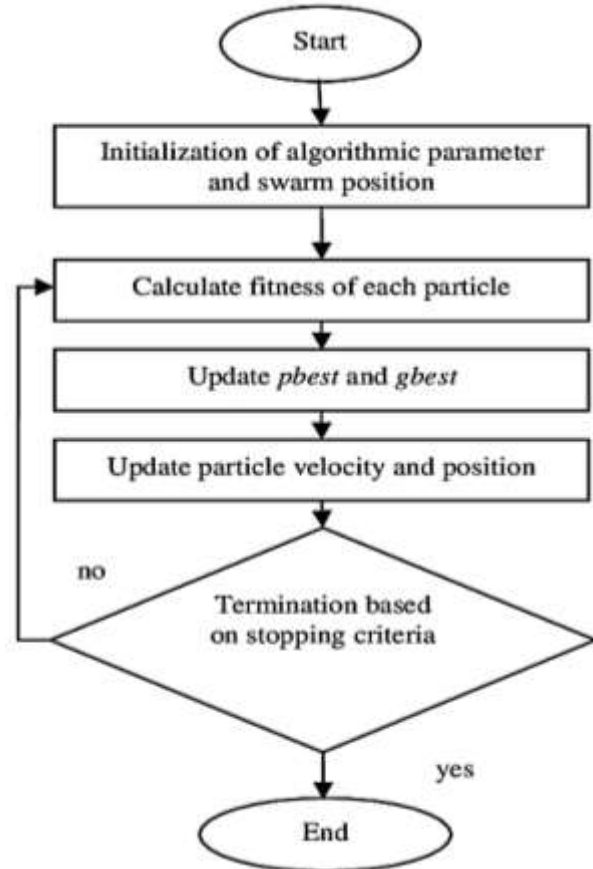


Fig. 5 Flowchart of particle swarm optimization algorithm.

Table 2 Inputs of the bees optimization algorithm.

Parameters	Values
Number of particles (n_{swarm})	50
Weighting function (w)	$0.8 - (\text{Loop No.} / \text{Iteration No.}) * 0.45$
Cognitive coefficient (ϕ_p)	2
Social coefficient (ϕ_g)	2
Number of objective function calculation (I_{max})	2000

4 RESULTS AND DISCUSSION

The aim of current section is to present the results obtained from optimization of peeling stress in symmetric single-lap joint with two bees and particle swarm optimization algorithms. In order to validate the analytical solution, the dimensionless peeling stress distribution graphs ($\sigma_{3y}^u / P, \sigma_{3y}^l / P$) in the adhesive layer and adherends are compared by finite element solution presented in ref. [7] (“Fig. 6”). The selected

specifications for symmetric single-lap joint are given in “Table 3”.

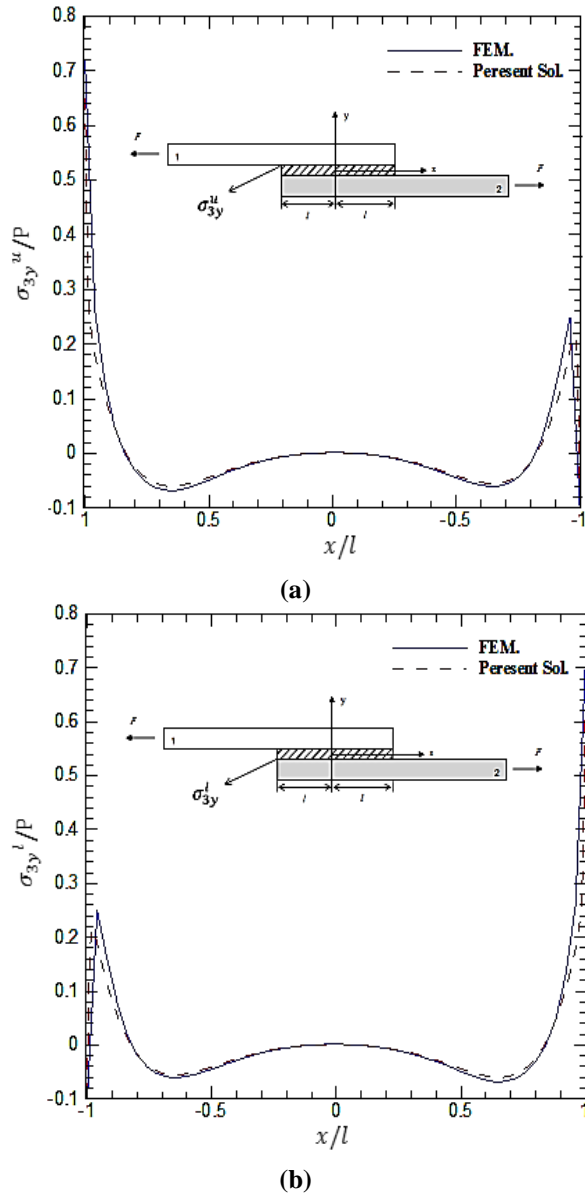


Fig. 6 Distribution of peeling stress in symmetric single-lap joint: (a): Top surface of adhesive layer, and (b): Bottom surface of adhesive layer.

Table 3 Properties of symmetric single-lap joint for comparison with finite element solution

Layer	Young's Modulus (GPa)	Poisson's Ration	Thickness (mm)	Length (mm)
Adherends	70	0.34	2	40
Adhesive	0.70	0.40	0.20	20

Based on “Fig. 6”, the trend of variation of graphs obtained from analytical and numerical solutions are in good agreement. According to this figure, the outcomes of finite element solution are slightly more cautious in comparison with analytical results. The reason for the existence of errors in the analytical solution is the assumptions applied in derivation of Equations. Assumptions used for symmetric state are: a) Shear stress along the adhesive thickness is constant and b) The adhesive layer cannot tolerate tensile force. The maximum error in the present method is 7%, which is reasonable. The results have very good agreement with finite element solution in all of the adhesive area. Comparison of the existing diagrams in Fig. 6 shows that the stress distribution at the top and bottom surface of the adhesive layer is opposite. The maximum stress value at the left side of the upper surface (“Fig. 6a”) and the right side of lower surface (“Fig. 6b”) occur and are numerically equal. The maximum stress concentration in the single-lap joint under the influence of tensile load is in these two regions and the reason is the existence of enhanced stress in the adherends.

4.1. Determining the Optimization Conditions for Single-Lap Adhesive Joint

Geometrical parameters affecting the distribution of peeling stress in symmetric single-lap joint which are chosen as design parameters which are: a) Thickness of adherends, Length and thickness of adhesive layer. The amount and range of the variation in the design parameters were selected according to the common dimensions used in previous studies and the samples used in the practical experiments. In all steps of optimization process, the objective function is single objective and the aim is to optimize the maximum peeling stress at the contact surface of adhesive and adherends. To investigate the amount of objective function, the value of peeling stress produced in the upper surface of the adhesive and the lower surface of the top adherend (σ_{3y}^u) is calculated. Then, the peeling stress was generated at the bottom surface of the adhesive and the top surface of the bottom adherend was calculated. Finally, the maximum peeling stress is created that is depended on the joint properties in one of these two areas considered as the objective function. The purpose of current study is to reduce the maximum objective function. The design variables and their range of changes for optimization of single-lap joint are presented in “Table 4”. It should be noted that the length of both adherends is 100 mm. In order to investigate the effect of adhesive and adherends material on the distribution of peeling stress, three types of adhesive and three different types of adherend were used. Adhesive No. 1 (Av138M-Epoxy) has a lower Young's modulus in comparison with adhesive No. 2 (Av2013-Epoxy) and No. 3 (DP8005-Epoxy).

This property is also considered as the criterion for selecting type of adhesive layer. The properties of adherends and adhesives are presented in “Table 5”.

Table 4 The selected range of parameters for optimization of symmetrical single-lap joint

Parameters	Min value (mm)	Max value (mm)
t_1	0.50	5
t_3	0.05	1
l	10	50

Table 5 Specifications of composite joint materials

Layers	Yield stress (MPa)	Poisson's ratio	Density (kg/m ³)	Young's modulus (GPa)
Adhesive No. 1	9.20	0.40	1065	0.50
Adhesive No. 2	34	0.37	1630	2.40
Adhesive No. 3	43	0.35	1700	2.70
Adherend No. 1 (Aluminum)	150	0.34	2700	70
Adherend No. 2 (Cast iron)	270	0.22	7200	140
Adherend No. 3 (Steel)	335	0.29	7800	210

4.2. Comparison of the Performance in BA and PSO

In this section, the comparison of BA and PSO algorithm has been studied in three different directions. Firstly, the value of objective function in the design range is compared. Then, the convergence rate and efficiency of two algorithms are investigated. The objective function values (maximum value of peeling stress in joint (σ_{3y}^{max})) were calculated by considering all three types of adhesive and using BA and PSO optimization algorithm. Based on “Table 6”, there is an acceptable overlap between the objective function values obtained from two optimization methods. It should be mentioned that the main inputs of BA and PSO optimization algorithm are given in “Tables 1 and 2”, respectively. The convergence of the two optimization algorithms for adhesive No. 1 is compared in “Fig. 7”. The convergence rate of BA and PSO algorithms is similar and the values of the objective function in both methods have converged after 20 iterations. As shown in “Fig. 7”, the BA diagram is more uniform than PSO algorithm. For this reason, the studies of variables have been performed based on the BA algorithm.

Table 6 Comparison of optimization results of BA and PSO algorithm in symmetrical composite joint.

Adhesive No	in BA σ_{3y}^{max} (MPa)	in PSO σ_{3y}^{max} (MPa)
1	1.67	1.67
2	2.11	2.11
3	2.98	2.99

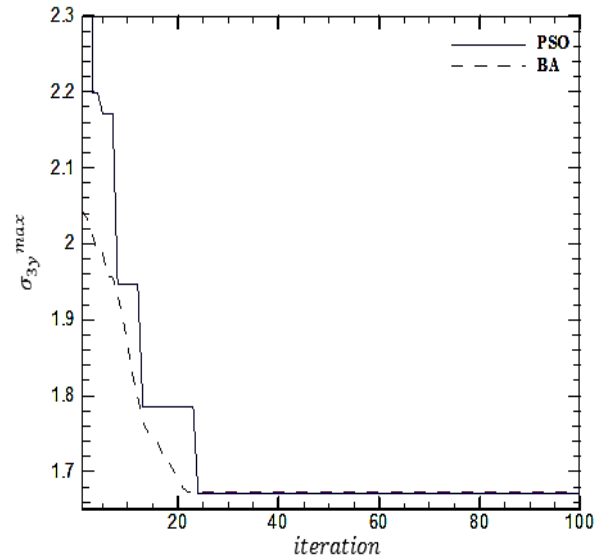


Fig. 7 Convergence of optimization algorithms for adhesive and adherend No. 1 in symmetric joint.

4.3. Optimal Values of Design Variables in Optimization

“Tables 4 and 5” have been used to determine the optimal values of the process variables, constant parameters and material specifications used in the symmetric composite single-lap joint. The optimal parameters obtained from the optimization process are presented in “Table 7”. The thickness of adherend layer and the length of the adhesive region parameters are in the maximum value of the design range for all cases. By increasing the length of the adhesive zone and the thickness of the adherends, the interlayer peeling stress decreases. The increase in the thickness of the adherend layer, due to the increase in the off-set of the load, is one of the causes of normal stresses between the layers. On the other hand, with the increase in the thickness of the adherends, the bending stiffness of the layers and, consequently, their strength to the bending moment and the resulting peeling stress increase. Increasing the length of the adhesive region also increases the capacity to bear stress in the adhesive layer and prevents the intensification of the effect of stress concentration in the edges on each other.

Table 7 Results of optimization of process parameters in symmetric single-lap joint.

	Type of adhesive	t ₁ (mm)	t ₂ (mm)	t ₃ (mm)
Adherend No. 1	No. 1	5	0.19	100
	No. 2	5	0.27	100
	No.3	5	0.24	100
Adherend No. 2	No. 1	5	0.15	100
	No. 2	5	0.24	100
	No.3	5	0.27	100
Adherend No. 3	No. 1	5	0.13	100
	No. 2	5	0.22	100
	No.3	5	0.26	100

4.4. Effect of the Adhesive Region Length in The Design Range

The diagrams of the maximum peeling stress changes versus the adhesive zone length for different adhesives are presented in “Fig. 8”.

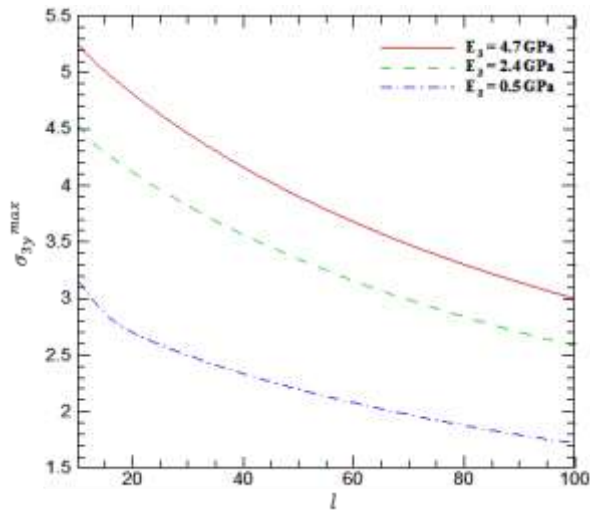


Fig. 8 The effect of the adhesive zone length on the maximum peeling stress for different adhesives in single-lap composite joint.

Increasing the length of the adhesive zone in the design range for all three types of adhesives has almost led to 45% reduction in the maximum value of the peeling stress in the joint. The hardening of the adhesive layer is one of the main factors for increasing the peeling stress in the composite joint. The reason is that adhesives transfer stress in shearing form. When one of the layers is subjected to a tensile load, this load is transferred to the adhesive in the form of shear stress

and the length of the adhesive is increased so much that it is able to transfer all load to the second layer. Hardening of the Young's modulus of the adhesive reduces its flexibility and as a result, the concentration of stress in the edges increases. When the Young's modulus of the adhesive increases, due to the increase in hardness, the adhesive is not able to transfer stress to its middle regions, and this leads to a decrease in the quality of the structure. It should be mentioned that increasing the hardness of the adhesive layer helps to balance the stress ratio on the edges. Although reducing the Young's modulus of the adhesive is a suitable path to reduce the peeling stress at the edges of the adhesive area, due to the increase in the length of the adhesive, there is a possibility of reaching the failure strain. For this reason, such adhesives are not suitable for large loads. The effect of the adhesive zone length on the maximum peeling stress in the joint for different adherends is shown in “Fig. 9”, in which adhesive No. 1 is used.

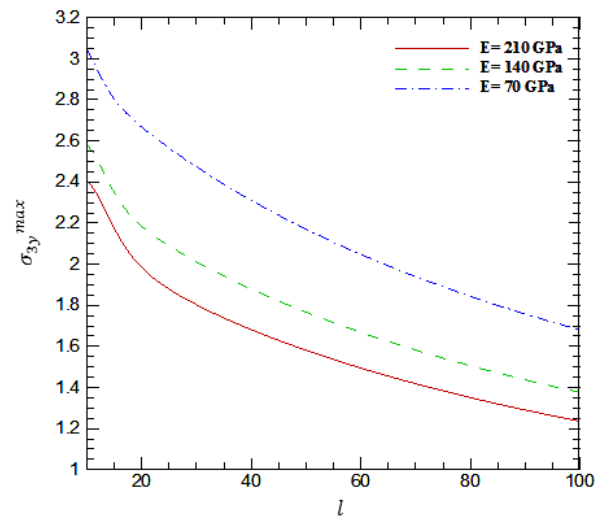


Fig. 9 The effect of the adhesive zone length on the maximum peeling stress for different adherends in single-lap composite joints.

The effect of Young's modulus of adherends is the opposite of the Young's modulus of the adhesive layer. Increasing Young's modulus of adherends increases their bending stiffness. The hardening of the adherends makes them more resistant to peeling stress and prevents the deformation of the layers in the vertical direction. In adherends with Young's modulus and high strength, the peeling stress in the joint is negligible and can be ignored.

4.5. The Effect of Adherend Thickness in The Design Range

The effect of changes in the thickness of the adhesive layer on the maximum peeling stress changes for

different adhesives and adherends are shown in “Figs. 10 and 11”, respectively.

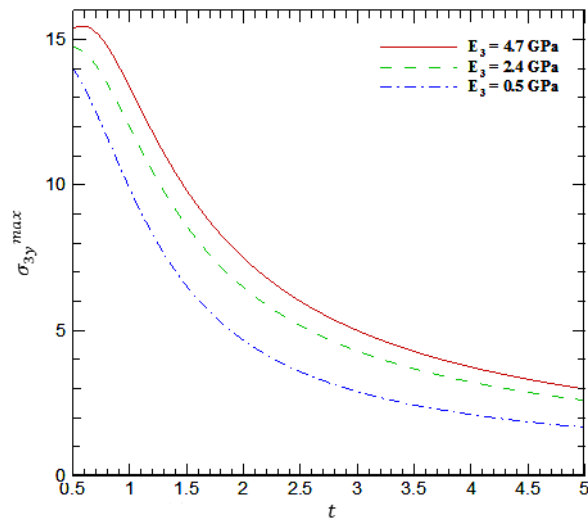


Fig. 10 The effect of adhesived layer thickness on the maximum peeling stress for different adhesives in single-lap composite joint.

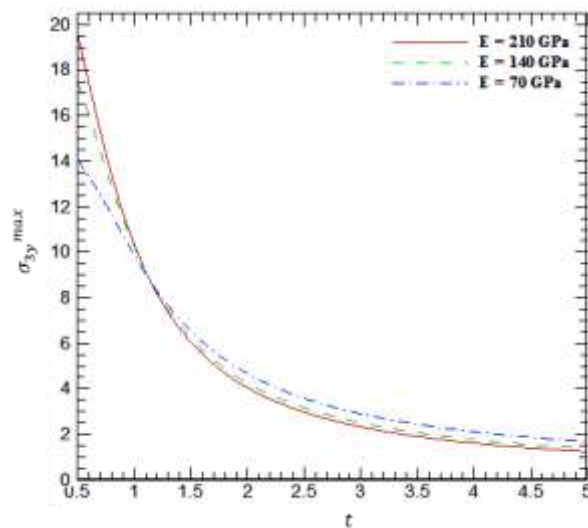


Fig. 11 The effect of adhesived layer thickness on the maximum peeling stress for different adherends in single-lap composite joint.

Increasing the thickness of the adherends leads to a decrease in the peeling stress in the composite joint. Comparison of “Figs. 8 and 9” with “Figs. 10 and 11” demonstrates that the effect of increasing the adherend thickness on the reduction of peeling stress is much greater than the effect of increasing the length of the adhesive region. As can be seen, when the thickness of the adherend layer is equal to 1.1 mm, the maximum peeling stress has been obtained unique for all three types of adhesives. In the present research work, when the thickness of the adherend is less than this value,

using an adherend with a higher Young's modulus leads to an increase in the peeling stress in the joint. The results are similar for thicknesses greater than 1.1 mm. For thicknesses greater than 1.1 mm, the results will be the opposite.

4.6. The Effect of The Thickness of The Adhesive Layer in The Design Range

The behavior of the adhesive zone length and the thickness of the adherends in the symmetric composite single-lap joint were investigated. The purpose of this section is to study the effect of the adhesive layer thickness (t_3) on the peeling stress in symmetrical joints. In the design of the adhesive joint, choosing an appropriate thickness and material of the adhesive is of great importance. The reason for this is that in most cases, it is not possible to easily change the thickness and materials of the adherends layers. Increasing the length of the adhesive zone is also limited. The curve of maximum peeling stress changes in terms of adhesive layer thickness for different adhesives is shown in “Fig. 12”.

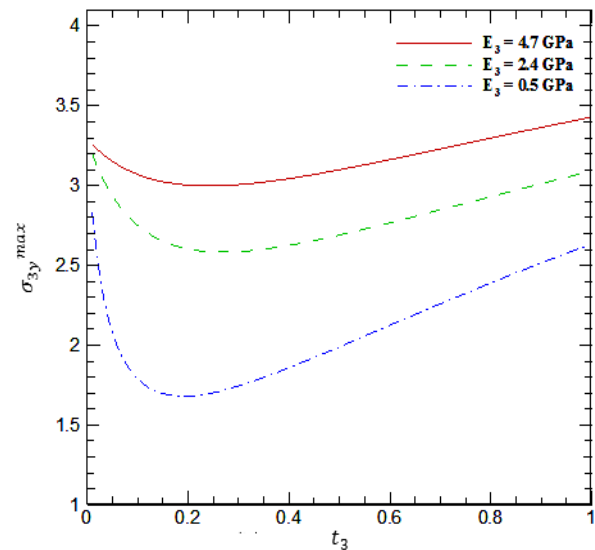


Fig. 12 The effect of adhesive layer thickness on maximum peeling stress for different adhesives.

The effect of Young's modulus of adhesives on the maximum value of peeling stress in the composite joint is almost similar to what was checked for the previous parameters. In design ranges, the adhesive with higher Young's modulus creates more peeling stress in the joint, but the trend of the stress changes for different adhesives is dissimilar, apart from its size. By increasing the thickness of adhesive No. 1, the maximum value of the peeling stress reaches from 2.8 MPa to 1.7 MPa (minimum value) in the adhesive thickness equal to 0.19 mm. These values were calculated as 3.2 MPa, 2.6 MPa and 0.27 mm for adhesive No. 2 and 3.3 MPa, 3 MPa and 0.24 mm for

adhesive No. 3, respectively. The values obtained from the above graphs show that within the design range of adhesive thickness, adhesive No 1 is more sensitive to thickness changes. Figure 13 shows the effect of adhesive thickness on the maximum peeling stress for different adherends.

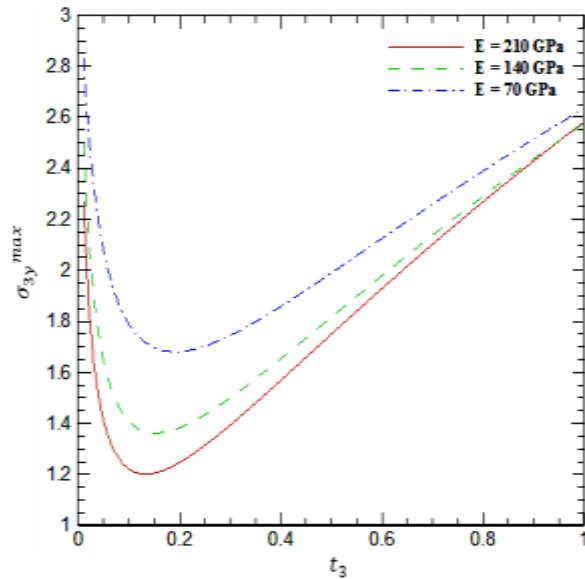


Fig. 13 The effect of adhesive layer thickness on maximum peeling stress for different adherends.

All adhesives have shown almost similar behavior in the range of adhesive thickness changes. At the end of the adhesive thickness design range, the same values for the maximum peeling stress have been obtained (about 2.6 MPa), but at the optimal point, this difference reaches its maximum. As shown in “Fig. 13”, the optimal stress in adherend No. 1 (1.7 MPa) is about 40% higher than adherend No. 3 (1.2 MPa). The optimal adhesive points for adherends No. 1, No. 2, and No. 3 are 0.19 mm, 0.15 mm, and 0.13 mm, respectively.

4.7. Choosing the Appropriate Adhesive

In this section, the effect of the thickness and material of the adhesive layer has been examined. In addition to the maximum peeling stress, its distribution in the adhesive area has also been discussed, so that finally the appropriate adhesive can be selected based on the needs of the designer. Figures 14 and 15 show the effect of adhesive hardness on the distribution of peeling stress in the upper and lower surface of the adhesive layer, respectively. In “Table 8”, a comparison is presented for different adhesives in order to evaluate the distribution of peeling stress on the upper surface of the adhesive. Due to the symmetry of the composite joint, the presentation of this table is omitted for the bottom surface.

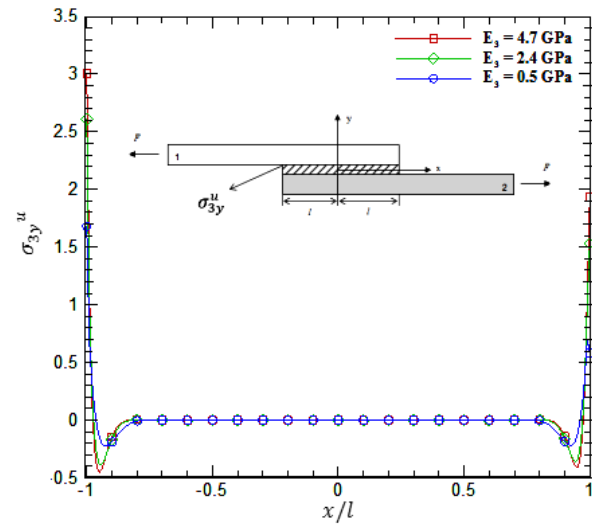


Fig. 14 The effect of adhesive Young's modulus on the optimized peeling stress distribution in the upper surface of the adhesive layer.

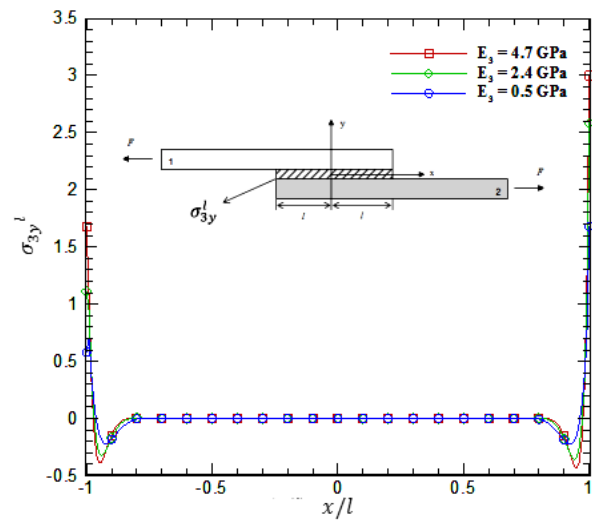


Fig. 15 The effect of adhesive Young's modulus on the optimized peeling stress distribution in the lower surface of the adhesive layer.

Table 8 Comparison of peeling stress in different adhesives.

Type of adhesive layer	Stress on the right edge (MPa)	Stress on the left edge (MPa)	Left to right stress ratio
No. 1	0.6	1.7	2.8
No. 2	1.5	2.6	1.7
No. 3	1.9	3.0	1.5

The results presented in current table are for adherend No. 1 (aluminum). The results obtained from the mentioned table revealed the harder adhesive layer, although it causes more peeling stress, but it makes the ratio of stress in the edges more uniform. To reduce the stress concentration, the end edges (which are prone to

stress concentration) can be filled with soft adhesives and other areas with hard adhesives (which are stronger). This type of design can increase the bearing load capacity of the joint.

In the present study, the adhesive layer consists of only one type of adhesive. In this type of design, depending on the amount of the load, the material and the thickness of the layers, the adhesive is selected, which will be discussed further.

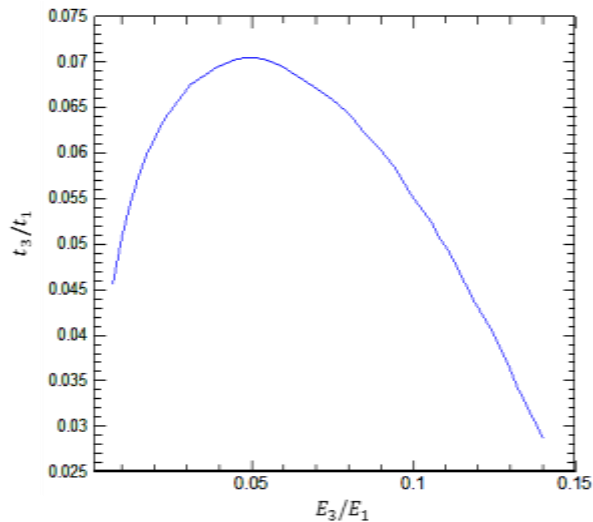


Fig. 16 The effect of Young's modulus ratio of adhesive to adherend on optimal thickness of adhesive to adherend ratio.

With the increase of the hardness ratio of the adhesive to the adherend, the thickness ratio firstly starts to increase and reaches its maximum value at 0.05. Then, the optimal thickness of the adhesive layer tends to zero at high ratios of Young's modulus of the adhesive to the adherend. These results demonstrate that choosing an adhesive with a very low or very high Young's modulus leads to the design of a composite joint (if the optimal point of adhesive thickness is used) with a small thickness of the adhesive layer. It should be mentioned that the main purpose of designing an adhesive joint is to transfer force in the form of shear stress and the thickness chosen for the adhesive layer, in addition to minimizing the peeling stress, should not lead to the concentration of shear stress in the adhesive. In order to present the design of sing-lap joint based on the minimization of the peeling stress and limiting the shear stress, the behavior of the shear stress in the adhesive layer is briefly investigated. By approaching the maximum value of the curve in the mentioned figure (by choosing the Young's modulus of the adhesive to the adherend ratio equal to 0.05, the thickest optimal value of the adhesive to the adherend layer is obtained), in addition to minimizing the peeling stress in the joint, the concentration of shear stress in the adhesive is also reduced. This choice is more

practical for soft adherends such as aluminum. When the adherend Young's modulus is high, this choice is not suitable and practical. Here, the hardness factor of the adhesive layer and the optimal point of its thickness ratio should be evaluated together and the most suitable adhesive should be selected. In order to design a symmetrical joint based on minimizing the peeling stress in the composite joint, the optimal thickness of the adhesive and its material should be selected based on "Fig. 16" in such a way that soft adhesive is used as much as possible and also the optimal thickness obtained is not too small for the adhesive layer.

Based on the outcomes of this section, for soft adherends (Young's modulus below 100 GPa), it is suitable to use the thickness of the adhesive layer between 0.1 mm and 0.15 mm and the E for the adhesive between 0.5 GPa to 1 GPa. For hard adherends (between 100 GPa and 200 GPa), the thickness of the adhesive is between 0.15 mm and 0.25 mm and the Young's modulus is 1 GPa to 3 GPa. Also, the results in present research work show that for small loads (less than 1000 N), the lowest value of E for the adhesive layer is selected as much as possible, and for large loads (more than 4000 N) avoid choosing soft adhesives.

5 CONCLUSIONS

In current research work, the optimization of the stress caused by the peeling effect in symmetrical single-lap composite joints was investigated. In the presented analytical solution, two-dimensional elasticity theory, stress-strain relations and also strain-displacement have been applied to investigate the stress distribution in the joint layers. In order to perform the optimization operation, bees and particle swarm optimization algorithms were used and their accuracy and convergence speed were compared. Then, the influences of geometrical factors such as thickness and length in the adhesive area as well as the type of adhesive and adherends on the peeling stress were studied. The results of present study are summarized below:

- The bees optimization algorithm is more accurate compared to the particle swarm algorithm and requires less repetition to reach the solution. PSO algorithm has a higher execution speed, but stops at local optima more often.
- In the symmetric composite single-lap joint, the increase in the length of the adhesive zone and the thickness of the adherends, leads to a decrease in the inter-layer peeling stress in the adhesive area.
- Among the three parameters affecting the peeling stress, there is an optimal thickness in the design range for the adhesive layer, where the peeling

stress between the adhesive layer and the bonded layer is minimized. This thickness depends on the type of adhesive layer and adherends as well as their thickness.

- An increase in Young's modulus of the adhesive layer leads to an increase in the peeling stress within the design range of the length of the adhesive area and the thickness of the adherends. In the design range of the thickness of the adhesive layer, changing the Young's modulus of the adhesive leads to change in the optimal point of its thickness, but the adhesive with a higher Young's modulus still creates a higher peeling stress in the composite joint.
- Increasing the Young's modulus of adherends within the design range of the adhesive region length and the adhesive layer thickness leads to reduction in the peeling stress. In the design range of adherends thickness and in very small thicknesses, the increase in Young's modulus of adherends leads to an increase in peeling stress, and with the increase of the adherends thickness (when it becomes more than 1.1 mm), this effect is reversed.
- The optimal point of the adhesive layer thickness depends on the Young's modulus of the adhesive to the adherend ratio, and at the Young's modulus ratio equal to 0.05, the optimal ratio of the thickness of the adhesive to the adherend reaches to its maximum value (equal to 0.07).

REFERENCES

- [1] Lee, J., Bae, D., Chung, W., Kim, K., Lee, J., and Cho, Y., Effects of Annealing on the Mechanical and Interface Properties of Stainless Steel/Aluminum/Copper Clad-Metal Sheets, *Journal of Materials Processing Technology*, Vol. 187, 2007, pp. 546-549, <https://doi.org/10.1016/j.jmatprotec.2006.11.121>.
- [2] Li, L., Nagai, K., and Yin, F., Progress in Cold Roll Bonding of Metals, *Science and Technology of Advanced Materials*, Vol 9, No. 2, 2008, pp. 023001, <https://doi.org/10.1088/1468-6996/9/2/023001>.
- [3] Manesh, H. D., Shahabi, H. S., Effective Parameters on Bonding Strength of Roll Bonded Al/St/Al Multilayer Strips, *Journal of Alloys and Compounds*, Vol. 476, No. 1-2, 2009, pp. 292-299, <https://doi.org/10.1016/j.jallcom.2008.08.081>.
- [4] Shishehsaz, M., Yaghoubi, S., The Effect of Fiber Breakage on Transient Stress Distribution in a Single-Lap Joint Composite Material, *Journal of Solid Mechanics*, Vol. 7, No. 4, 2015, pp. 442-57, <https://dorl.net/dor/20.1001.1.20083505.2015.7.4.6.3>.
- [5] Hart-Smith, L., Design of Adhesively Bonded Joints, Elsevier Applied Science Publishers Ltd, Joining Fibre-Reinforced Plastics, 1987, pp. 271-311.
- [6] Molitor, P., Barron, V., and Young, T., Surface Treatment of Titanium for Adhesive Bonding to Polymer Composites: A Review, *International Journal of Adhesion and Adhesives*, Vol. 21, No. 2, 2001, 129-136, [https://doi.org/10.1016/S0143-7496\(00\)00044-0](https://doi.org/10.1016/S0143-7496(00)00044-0).
- [7] Zhao, B., Lu, Z. H., A Two-Dimensional Approach of Single-Lap Adhesive Bonded Joints, *Mechanics of Advanced Materials and Structures*, Vol. 16, No. 2, 2009, pp. 130-59, <https://doi.org/10.1080/15376490802625464>.
- [8] Bavi, O., Bavi, N., and Shishesaz, M., Geometrical Optimization of the Overlap in Mixed Adhesive Lap Joints, *The Journal of Adhesion*, Vol. 89, No. 12, 2013, pp. 948-972 <https://doi.org/10.1080/00218464.2013.782813>.
- [9] Shishehsaz, M., Moradi, S., and Yaghoubi, S., Transient Stress Analysis In Adhesive Single Lap Joints of a Composite Material Due To Fiber Breakage, *Journal of Solid and Fluid Mechanics*, Vol. 4, No. 4, 2015, pp. 113-126, <https://doi.org/10.22044/jsfm.2015.398>.
- [10] Selahi, E., Semi Analytical Transient Dynamic Analysis of Composite Adhesive Single-lap Joints, *Mechanics of Advanced Composite Structures*, Vol. 7, No. 1, 2020, pp. 137-145, <https://dx.doi.org/10.22075/mac.2019.16036.1161>,
- [11] Wang, S., Liang, W., Duan, L., Li, G., and Cui, J., Effects of Loading Rates on Mechanical Property and Failure Behavior of Single-Lap Adhesive Joints with Carbon Fiber Reinforced Plastics and Aluminum Alloys, *The International Journal of Advanced Manufacturing Technology*, Vol. 106, No. 5, 2020, pp. 2569-2581, <https://doi.org/10.1007/s00170-019-04804-w>.
- [12] de Miguel, A., Pagani, A., Rizzo, L., Catapano, A., and Panettieri, E., Accurate Evaluation of 3D Stress Fields in Adhesive Bonded Joints Via Higher-Order FE Models, *Mechanics of Advanced Materials and Structures*, Vol. 27, No. 4, 2020, pp. 333-345, <https://doi.org/10.1080/15376494.2018.1472352>.
- [13] Polini, W., Corrado, A., Effect of Adherends Misalignment on the Strength of Single-Lap Bonded Joints, *The International Journal of Advanced Manufacturing Technology*, Vol. 106, No. 3, 2020, pp. 817-828, <https://doi.org/10.1007/s00170-019-04652-8>.
- [14] Beigrezaee, M., Ayatollahi, M., Bahrami, B., and Da Silva, L., A New Geometry for Improving the Strength of Single-Lap Joints Using Adherend Notching Technique, *The Journal of Adhesion*, Vol. 97, No. 11, 2021, pp. 1004-1023, <https://doi.org/10.1016/j.tafmec.2022.103364>.
- [15] Peres, L., Arnaud, M., Silva, A., Campilho, R., Machado, J., and Marques, E., Geometry and Adhesive Optimization of Single-Lap Adhesive Joints Under Impact, *The Journal of Adhesion*, Vol. 98, No. 6, 2022, pp. 677-703, <https://doi.org/10.1080/00218464.2021.1994404>.
- [16] Marchione, F., Effect of Hollow Adherends on Stress Peak Reduction in Single-Lap Adhesive Joints: FE and Analytical Analysis, *The Journal of*

- Adhesion, Vol. 98, No. 6, 2022, pp. 656-676, <https://doi.org/10.1080/00218464.2021.1995368>.
- [17] Zhao, B., Lu, Z. H., and Lu, Y. N., Closed-Form Solutions for Elastic Stress–Strain Analysis in Unbalanced Adhesive Single-Lap Joints Considering Adherend Deformations and Bond Thickness, *International Journal of Adhesion and Adhesives*, Vol. 31, No. 6, 2011, 434-445, <https://doi.org/10.1016/j.ijadhadh.2011.03.002>.
- [18] Cheng, S., Chen, D., and Shi, Y., Analysis of Adhesive-Bonded Joints with Nonidentical Adherends, *Journal of Engineering Mechanics*, Vol. 117, No. 3, 1991, pp. 605-623, [https://doi.org/10.1061/\(ASCE\)0733-9399\(1991\)117:3\(605\)](https://doi.org/10.1061/(ASCE)0733-9399(1991)117:3(605)).
- [19] Pham, D., Ghanbarzadeh, A., Otri, S., and Koç, E., Optimal Design of Mechanical Components Using the Bees Algorithm, *Proceedings of the Institution of Mechanical Engineers, Part C: Journal of Mechanical Engineering Science*, Vol. 223, No. 5, 2009, pp. 1051-1056, <https://doi.org/10.1243/09544062JMES838>.
- [20] Zhou, C., Gao, H., Gao, L., and Zhang, W., Particle Swarm Optimization (PSO) Algorithm, *Application Research of Computers*, Vol. 12, 2003, pp. 7-11.